

# Elucidation of the Molecular Mechanisms of Protein Folding

Department of Life and Coordination-Complex Molecular Science  
Division of Biomolecular Functions



KUWAJIMA, Kunihiro  
MAKABE, Koki  
NAKAMURA, Takashi  
CHEN, Jin  
TAKENAKA, Toshio  
MIZUKI, Hiroko  
IKEDA, Yukako  
TANAKA, Kei

Professor  
Assistant Professor  
IMS Research Assistant Professor  
OIB Research Assistant Professor  
Post-Doctoral Fellow  
Technical Fellow  
Technical Fellow  
Secretary

Kuwajima group is studying mechanisms of *in vitro* protein folding and mechanisms of molecular chaperone function. Our goals are to elucidate the physical principles by which a protein organizes its specific native structure from the amino acid sequence. In this year, we studied the equilibrium and kinetics of bimolecular  $\text{MgATP}^{2-}$  binding to GroEL.

## 1. Dissecting a Bimolecular Process of $\text{MgATP}^{2-}$ Binding to the Chaperonin GroEL

The chaperonin GroEL from *Escherichia coli*, a tetradecameric protein complex consisting of two heptameric rings stacked back to back with a central cavity, is one of the best characterized molecular chaperones that facilitate protein folding *in vivo*. The  $\text{ATP}^-$  dependent control of the affinity for its target protein and the co-chaperonin GroES is essential for its molecular chaperone function, and this control occurs through a series of cooperative allosteric transitions of GroEL induced by  $\text{MgATP}^{2-}$ . The equilibria and kinetics of the allosteric transitions of GroEL have thus been studied for some time by a variety of techniques. However, the initial bimolecular step of  $\text{MgATP}^{2-}$  binding to GroEL, which must precede the allosteric transitions, remains to be clarified.

Here, we studied the equilibrium and kinetics of  $\text{MgATP}^{2-}$  binding to a variant of GroEL, in which Tyr485 was replaced by tryptophan, via isothermal titration calorimetry (ITC) and stopped-flow fluorescence spectroscopy (Figures 1 and 2). In the absence of  $\text{K}^+$  at 4 ~ 5 °C, the allosteric transitions and the subsequent ATP hydrolysis by GroEL are halted, and hence, the stopped-flow fluorescence kinetics induced by rapid mixing of  $\text{MgATP}^{2-}$  and the GroEL variant solely reflected  $\text{MgATP}^{2-}$  binding, which was well represented by bimolecular noncooperative binding with a binding rate constant,  $k_{\text{on}}$ , of  $9.14 \times 10^4 \text{ M}^{-1} \text{ s}^{-1}$  and a dissociation rate constant,  $k_{\text{off}}$ , of  $14.2 \text{ s}^{-1}$ , yielding a binding constant,  $K_{\text{b}} (= k_{\text{on}}/k_{\text{off}})$ , of  $6.4 \times 10^3 \text{ M}^{-1}$ . We also successfully performed ITC to measure

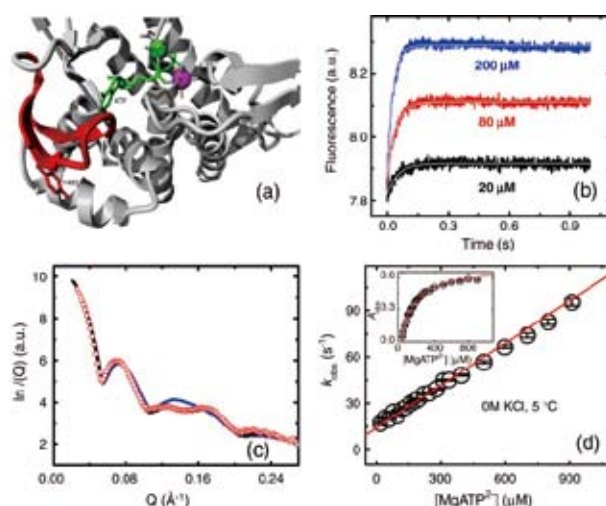


**Figure 1.** The structure around the  $\text{MgATP}^{2-}$ -binding site of GroEL (a), the SAXS patterns of wild-type GroEL in the different allosteric states (b), and the binding kinetics of  $\text{MgATP}^{2-}$  to GroEL(Y485W) (c and d).

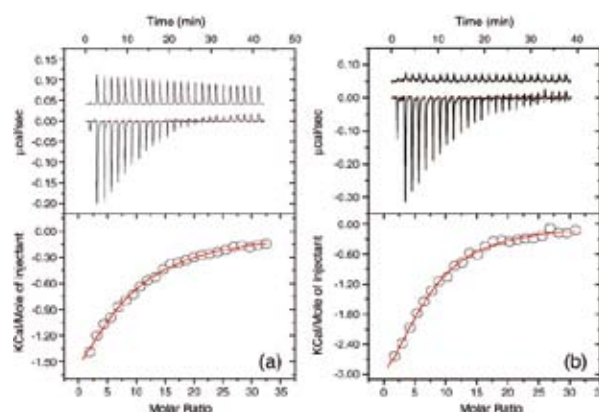


**Figure 2.**  $\text{MgATP}^{2-}$ -binding isotherms to GroEL(Y485W) (a) and GroEL(wild type) (b) measured by ITC in the absence of  $\text{K}^+$  at 5 °C.

binding isotherms of  $\text{MgATP}^{2-}$  to GroEL and obtained a  $K_b$  of  $9.5 \times 10^3 \text{ M}^{-1}$  and a binding stoichiometric number of 6.6 (Figure 2).  $K_b$  was thus in good agreement with that obtained by stopped-flow fluorescence. In the presence of 10 ~ 50 mM KCl, the fluorescence kinetics consisted of three to four phases (the first fluorescence-increasing phase, followed by one or two exponential fluorescence-decreasing phases, and the final slow fluorescence-increasing phase), and comparison of the kinetics in the absence and presence of  $\text{K}^+$  clearly demonstrated that the first fluorescence-increasing phase corresponds to bimolecular  $\text{MgATP}^{2-}$  binding to GroEL. The temperature dependence of the kinetics indicated that  $\text{MgATP}^{2-}$  binding to GroEL was activation-controlled with an activation enthalpy

as large as 14 ~ 16 kcal mol<sup>-1</sup>.

To further elucidate what kind of activation ( $\text{P}^*\text{L} \rightarrow \text{PL}^\ddagger$ ) takes place during  $\text{MgATP}^{2-}$  binding to apo GroEL, we investigated the X-ray crystallographic structures of the  $\text{MgATP}^{2-}$ -binding site of apo GroEL (PDB code: 1OEL) and  $\text{MgATP}^{2-}$ -bound GroEL (PDB code: 1KP8). The  $\text{MgATP}^{2-}$ -bound GroEL, originally complexed with ATP $\gamma$ S, assumed the T-state conformation, and hence provides an excellent model of the  $\text{MgATP}^{2-}$ -bound complex (PL) in the present study. As a result, the two structures were almost superimposable to each other. All atoms other than the O $\gamma$  of Thr38 are not shifted more than 1.9 Å (Figure 3(a)).

If there is no essential difference in the binding-site structure between apo and  $\text{MgATP}^{2-}$ -bound GroEL, how can we explain the  $\Delta H^\ddagger$  of 14 ~ 16 kcal mol<sup>-1</sup> that is involved in the activation step from  $\text{P}^*\text{L}$  to PL (Figure 3(b))? A possible explanation is given by partial dehydration and conformational strain in the transition-state complex ( $\text{PL}^\ddagger$ ) that exists between  $\text{P}^*\text{L}$  and PL. Both  $\text{MgATP}^{2-}$  and the binding groove of GroEL are highly hydrated in  $\text{P}^*\text{L}$ , but these hydrated water molecules must be completely removed from the binding surface between  $\text{MgATP}^{2-}$  and the binding groove in PL, except for the two caves underneath the groove. In  $\text{PL}^\ddagger$ ,  $\text{MgATP}^{2-}$  and the binding groove are thus only partially dehydrated, and this partial dehydration increases the energy level of  $\text{PL}^\ddagger$  as the final stabilization requires full dehydration. Furthermore, there may be conformational strain imposed on the binding groove in  $\text{PL}^\ddagger$  when specific interactions steer the ligand into the binding groove, and probably some openings at the entrance of the groove are required for accommodating  $\text{MgATP}^{2-}$ . Such conformational strain also increases the energy level of  $\text{PL}^\ddagger$ . As a result, the activation from  $\text{P}^*\text{L}$  to PL is accompanied by a  $\Delta H^\ddagger$  as large as 14 ~ 16 kcal mol<sup>-1</sup>. Interestingly, a very similar  $\Delta H^\ddagger$  (16 kcal mol<sup>-1</sup>) was observed in the reversed activation from  $\text{P}^*\text{L}$  to PL. In the reversed process, the partial hydration and the conformational strain similarly occur in  $\text{PL}^\ddagger$ , leading to the similar  $\Delta H^\ddagger$  in the reversed activation process.

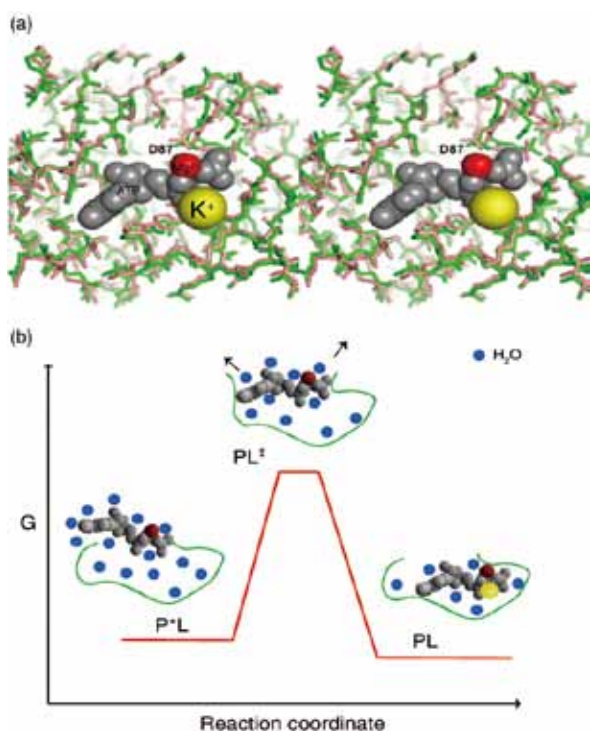


**Figure 3.** (a) A stereo view of superposition of X-ray structures of apo GroEL (green) (PDB code: 1OEL) and  $\text{MgATP}^{2-}$ -bound GroEL (pink) (PDB code: 1KP8) in a region around the binding site. (b) A reaction diagram of  $\text{MgATP}^{2-}$  binding to GroEL and schematic representations for the diffusional encounter complex ( $\text{P}^*\text{L}$ ), the transition-state complex ( $\text{PL}^\ddagger$ ), and the final stable complex (PL).

## Reference

- 1) J. Chen, K. Makabe, T. Nakamura, T. Inobe and K. Kuwajima, *J. Mol. Biol.* **410**, 343–356 (2011).